DOI: 10.1002/cbic.200500107

Access of the Substrate to the Active Site of Yeast Oxidosqualene Cyclase: An Inhibition and Site-Directed Mutagenesis Approach

Simonetta Oliaro-Bosso,[a] Tanja Schulz-Gasch,[b] Gianni Balliano,[a] and Franca Viola*[a]

A structural model of Saccharomyces cerevisiae *oxidosqualene cyclase (*Sce*OSC) suggests that some residues of the conserved sequence Pro-Ala-Glu-Val-Phe-Gly (residues 524–529) belong to a channel constriction that gives access to the active-site cavity. Starting from the* Sce*OSC C457D mutant, which lacks the cysteine residue next to the catalytic Asp456 residue Cys457 has been replaced but Asp456 is still there, we prepared two further mutants where the wild-type residues Ala525 and Glu526 were individually replaced by cysteine. These mutants, especially E526C, were very sensitive to the thiol-reacting agent dodecylmaleimide. Moreover, both the specific activity and the thermal stability of E526C were severely reduced. A similar decrease of the enzyme functionality was obtained by replacing Glu526 with alanine, while substitution with the conservative residues aspartate or glutamine did not alter catalytic activity. Molecular modeling of the yeast wild-type OSC and mutants on the template structure of human OSC confirms that the channel constriction is an important aspect of the protein structure and suggests a critical structural role for Glu526.*

Introduction

Oxidosqualene cyclases (OSCs, EC 5.4.99.7) catalyze a key reaction in sterol biosynthesis, the cyclization of oxidosqualene into different tetracyclic triterpenes, the precursors of phytosterols, cholesterol, and ergosterol.[1–3] Enzymatic cyclization of oxidosqualene has attracted the interest of researchers for decades, not only for its fascinating mechanism, the most complex among the monoenzymatic reactions, but also as a potential target in drug-development projects. Selective inhibition of OSCs has been considered, for instance, as a promising target for the control of blood cholesterol levels in humans[4–8] or for the treatment of severe diseases caused by pathogenic microorganisms.[9,10]

The first and for a long time the only crystallized protein belonging to the triterpene cyclase family has been the membrane enzyme *Alicyclobacillus acidocaldarius* squalene–hopene cyclase (*Aac*SHC), a bacterial counterpart of oxidosqualene cyclases.[11] *Aac*SHC has been used as a model for studying the mechanism of cyclization and the interactions of inhibitors with the active site.[12,13] Cocrystallization of *Aac*SHC with the substrate analogue 2-azasqualene has given the first direct evidence of how a squalene-like molecule is prefolded in the active site of a terpene cyclase enzyme.[14] Homology modeling studies, based on a comparison between *Aac*SHC and *Homo sapiens* oxidosqualene cyclase (*Hsa*OSC),[13] have provided a sound theory on the mechanism of stereoselective cyclization of oxidosqualene by *Hsa*OSC. Recently, the crystal structure of the *Hsa*OSC complex with both an inhibitor and the reaction product has been resolved, thereby allowing an insight into the active site and the cyclization mechanism of a lanosterol synthase.[15] The active site of *Hsa*OSC shares some important similarities with *Aac*SHC but also shows important differences, mainly in the catalytic mechanism which leads to the formation of a different final product.

Since the publication of the structure of *Aac*SHC[11] we have been interested in the problem of the access of the substrate into the active site. Crystallographic data suggest that the active site of *Aac*SHC is accessible from the interior side of the membrane through a nonpolar channel that contains a narrow constriction formed by four amino acid residues, one of which is a cysteine (Cys435, *Aac*SHC numbering). The involvement of this cysteine residue in the channel governing the access of the substrate has been shown by using thiol-reacting compounds to inhibit a mutated *Aac*SHC where the Cys435 was the only cysteine residue left. Different thiol-reacting compounds caused irreversible inhibition of the enzyme.[16] We interpreted these results as a consequence of the obstruction of the channel constriction by the inhibitors. Although absent in oxidosqualene cyclases, Cys435 belongs to a highly conserved sequence in triterpene cyclases (Figure 1), so it could be infer-

[a] *Dr. S. Oliaro-Bosso, Prof. G. Balliano, Prof. F. Viola*
Dipartimento di Scienza e Tecnologia del Farmaco
Facoltà di Farmacia, Università degli Studi di Torino
Via Pietro Giuria 9, 10125 Turin (Italy)
Fax: (+39) 011-6707695
E-mail: franca.viola@unito.it

[b] *Dr. T. Schulz-Gasch*
F. Hoffmann-La Roche Ltd., Molecular Design, PRBD-CS 92/2.10D
4010 Basel (Switzerland)

A. acidocaldarius SHC NHIPFCD-FG 438
S. cerevisiae OSC KAPLAMETLN--P-AEVFGNIMVEY 535
H. sapiens OSC RGGHLLELLN--P-SEVFGDIMIDY 528

Figure 1. Alignment of the sequences forming the hypothetic channel constriction of the SHC of *A. acidocaldarius* and of the OSCs of *S. cerevisiae* and *H. sapiens* (obtained with the MultAlin program).

red that such sequence should also contribute to the formation of a channel constriction in eukaryotic oxidosqualene cyclases.

In the crystallized *Hsa*OSC, the membrane-inserted surface indeed contains a channel separated from the active-site cavity by a constriction, and the conserved sequence of Figure 1 appears as a strained loop that could undergo a rearrangement allowing the substrate to access the active site.[15]

In the present work we have investigated the possible presence of a channel constriction in eukaryotic OSCs by preparing two mutants of *Saccharomyces cerevisiae* oxidosqualene cyclase (*Sce*OSC) in which two residues of the conserved sequence of the putative channel constriction (Ala525 and Glu526, yeast numbering) were separately replaced with a cysteine by site-directed mutagenesis. The Ala525 residue, corresponding in the aligned sequences to the *Aac*SHC Cys435 residue, appears from a structural model raised in homology with *Hsa*OSC to be located inward in the channel constriction, while the adjacent Glu526, although not protruding towards the hydrophobic channel, is completely conserved in all the eukaryotic OSCs, thus suggesting a possible structural role. In both cases, the substitution with cysteine residues allows the inhibition activity of thiol-reacting agents to be tested as a tool to investigate the role of these residues in determining the enzyme functionality.

The mutants were prepared from a *Sce*OSC mutant C457D, which lacks the Cys457 residue in the active site, in order to avoid interactions of the thiol-reacting inhibitors with this active-site residue. After observing that the mutation E526C significantly affected the catalytic activity, we prepared three further mutants where Glu526 was replaced respectively by aspartate, glutamine, and alanine, in order to study the role of this glutamate residue.

Results and Discussion

Modeling studies and characterization of *Sce*OSC mutants C457D, C457D–A525C, C457D–E526C, C457D–E526D, C457D–E526Q, and C457D–E526A

By using the recently published[15] structure of human OSC, a homology model of *Sce*OSC has been built in accordance with previously published homology models of *Hsa*OSC and *Arabidopsis thaliana* cycloartenol synthase (*Ath*CAS1) obtained by using *Aac*SHC as a template structure. Despite low sequence identity between *Hsa*OSC, *Ath*CAS1, and the template *Aac*SHC (pairwise percentage residue identity $<20\%$), reasonable explanations of mechanistic differences between the cyclases[13] and reliable predictions[17] have been made with these earlier homology models. The newly available template structure of *Hsa*OSC as a base for a homology model of *Sce*OSC should strongly increase the reliability and confidence in explanations drawn from the *Sce*OSC homology model (pairwise percentage residue identity $>40\%$).

As can be seen from Figure 2A, there are only a few major differences (sequence inserts and deletions) in the overall sequence alignment and these are mainly located at solvent-exposed positions of the structures. Thus, they do not affect catalysis, since the active site is deeply buried in the center of the

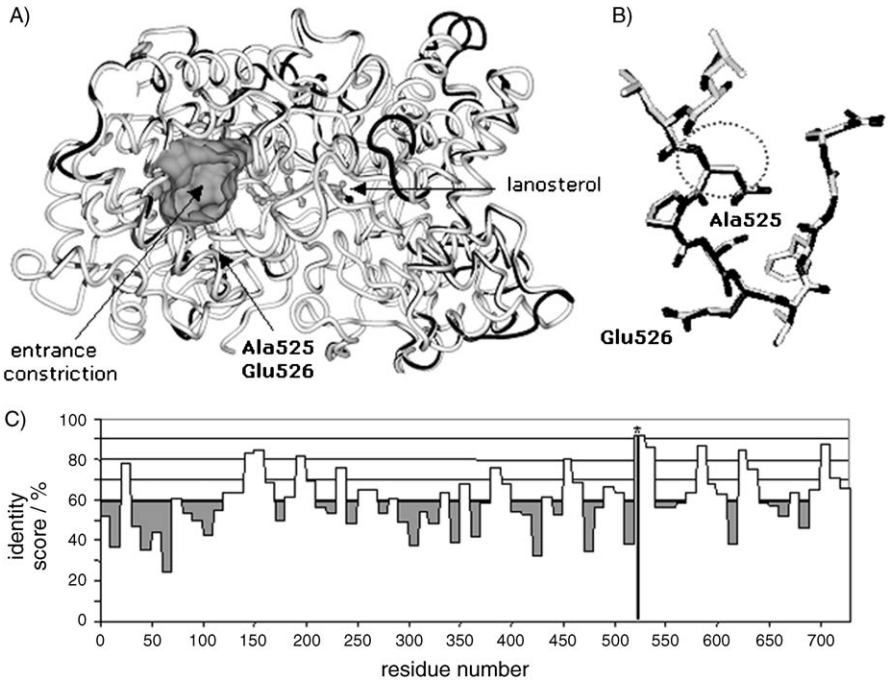

Figure 2. A) Superposition of the backbone of the crystal structure of *Hsa*OSC (gray) with the homology model of *Sce*OSC (black). Only where the black backbone is visible are there major differences (sequence inserts or deletions) between the human and yeast enzymes. Also shown are the entrance constriction, as a surface, the position of lanosterol in the active site, and the position of residues Ala525 and Glu526 of *Sce*OSC, which correspond to Ser518 and Glu519 of *Hsa*OSC. B) Superposition of structure fragments from human (gray) and yeast (black) OSCs containing residues Ala525 and Glu526. The constriction of the channel, formed in *Hsa*OSC by Tyr237, Ile524, and Cys233 (not shown),[15] is marked with a dotted circle. C) Sequence-identity score plot (average score calculated for a window of 10 residues). The gray background indicates the average identity score over the whole sequence alignment of human and yeast OSCs. The asterisk indicates the position of Ala525 and Glu526; this fragment is the most conserved part (score >90) of the two enzymes.

enzyme. Figure 2A also shows that there are no backbone changes caused by sequence inserts and deletions at the position of the entrance constriction. Figure 2B and C show that the sequence around the residues Ala525 and Glu526 (yeast numbering) is highly conserved. In fact, from the score plot in Figure 2C one can see that this part belongs to the most conserved section in the overall sequence alignment between human and yeast OSC (score >90). All these facts indicate that the yeast homology model around the constriction is very reliable.

By site-directed mutagenesis we first prepared a C457D mutant of the *ERG7* gene coding for *Sce*OSC, integrated into the *ERG7* defective strain SMY8.[18] This mutation involves the cysteine residue contiguous to the catalytic acid Asp456.[15] In *Hsa*OSC, the catalytic aspartate is assumed to be activated for the protonation step by the adjacent cysteine residue and by an additional active-site-located cysteine, Cys533.[15] The role of the cysteines is thus only secondary but could explain the previously described inhibition of yeast and mammalian OSCs by different thiol-reacting compounds.[19,20] In accordance with this putative secondary role of Cys457, the C457D mutant was indeed active, although less so than the wild-type OSC integrated into the SMY8 strain (SMY8[pSM61.21]). This mutant was used in the successive mutagenesis experiments to obtain C457D–A525C and C457D–E526C mutants, where the amino acids Ala525 and Glu526, corresponding to Cys435 of the channel constriction of *Aac*SHC and to the adjacent Asp436 residue, respectively, have been replaced by cysteine residues in order to test both the catalytic activity and the effect of thiol-reacting compounds. Sequence analysis of the three mutated *erg7* genes confirmed the presence and location of the mutations.

The transformation of the OSC defective yeast strain SMY8 with the mutated C457D, C457D–A525C, and C457D–E526C OSC genes abolished the sterol auxotrophy of the SMY8 strain: all three mutants, similarly to the SMY8 transformed with the wild-type OSC gene (SMY8[pSM61.21]), grew in the absence of ergosterol and biosynthesized labeled C_{27} sterols after incubation with [2-^{14}C]acetate for 4 h at 30 °C (Table 1). These results

Table 1. Incorporation of [2-^{14}C]acetate into nonsaponifiable lipids of the SMY8 yeast strain expressing wild-type and different mutant OSCs. Values are the means of duplicate assays of two different experiments.

*Sce*OSC mutant	Radioactivity incorporated into nonsaponifiable lipids / %				
	C_{27} sterols	lanosterol	dioxidosqualene	oxidosqualene	squalene
wild-type	68.6 ± 8.6	7.9 ± 2.1	1.9 ± 0.4	3.6 ± 2.1	18.0 ± 4.9
C457D	73.7 ± 4.7	7.3 ± 2.3	1.6 ± 1.0	2.4 ± 0.7	16.0 ± 6.3
C457D–A525C	86.2 ± 5.0	6.4 ± 2.2	2.4 ± 0.7	2.3 ± 1.2	2.7 ± 0.5
C457D–E526C	66.1 ± 4.9	16.6 ± 11.9	4.7 ± 0.9	5.8 ± 3.9	6.8 ± 2.2

are in agreement with those obtained with *Aac*SHC, where the mutation of the residues of the channel does not impair the catalytic activity.[16] In addition, mutagenesis studies by Corey et al. showed that mutation of Glu526 does not alter the viability of cells.[21]

Catalytic activity

The in vitro activity of the different *Sce*OSC mutants has been studied by using cell homogenates. Both squalene and oxidosqualene have been assayed as substrates for the C457D mutant, since this mutant has the same Asp-Asp-Thr-Ala-Glu sequence that is present in the active site of *Aac*SHC, where the two neighboring Asp residues are needed to protonate the substrate squalene.[3] In spite of the presence of the two contiguous Asp residues, squalene did not become a substrate for the C457D mutant. Thus, as already reported,[22] in eukaryotic oxidosqualene cyclases, the specific molecular recognition of the substrate oxidosqualene and the exclusion of squalene is not simply determined by the integrity of the substrate-protonating motif Asp-Cys-Thr-Ala. The mutation did not significantly affect the enzymatic activity, since the specific activity (1.28 nmol of oxidosqualene cyclized per hour per mg of proteins at 35 °C) was slightly lower than that of the wild-type SMY8[pSM61.21], a result confirming that the involvement of Cys457 should only be subsidiary. The activity of the C457D–A525C mutant under the same incubation conditions was similar, while the specific activity of mutant C457D–E526C after 1 h of incubation at 35 °C was 10 times lower (Table 2).

Table 2. OSC specific activity [nanomoles of substrate transformed per h per mg of protein] of the homogenates of the differently transformed SMY8 strains. Values are the means of duplicate assays of at least two different experiments.

*Sce*OSC mutant	Specific activity / nmol h^{-1} per mg protein	
	35 °C	25 °C
wild-type	1.75 ± 0.24	1.03 ± 0.14
C457D	1.28 ± 0.16	0.38 ± 0.12
C457D–A525C	1.26 ± 0.17	0.68 ± 0.31
C457D–E526C	0.15 ± 0.08	0.090 ± 0.04
C457D–E526D	0.77 ± 0.05	0.52 ± 0.08
C457D–E526Q	1.15 ± 0.26	0.58 ± 0.24
C457D–E526A	0.29 ± 0.13	0.092 ± 0.02

Figure 3A shows that the amount of product formed by mutant C457D–E526C did not increase during 6 h of incubation at 35 °C but slowly increased at 25 °C. After 6 h at 25 °C, we could obtain about the same amount of product as after 1 hour with mutant C457D–A525C at 35 °C. The activity of C457D–E526C was significantly decreased by preincubation at 35 °C in the absence of substrate. After 4 h at 35 °C the activity was almost completely lost, while the activity of mutant C457D under the same conditions was not affected (Figure 3B). The mutation of Glu526 thus affects both catalytic activity and thermal stability.

The crystal structure of *Hsa*OSC in combination with the homology model of *Sce*OSC allows explanations for the abovementioned experimental observations. The double mutant C457D–A525C shows unchanged specific activity (Table 2) compared to the single mutant C457D. As can be seen from

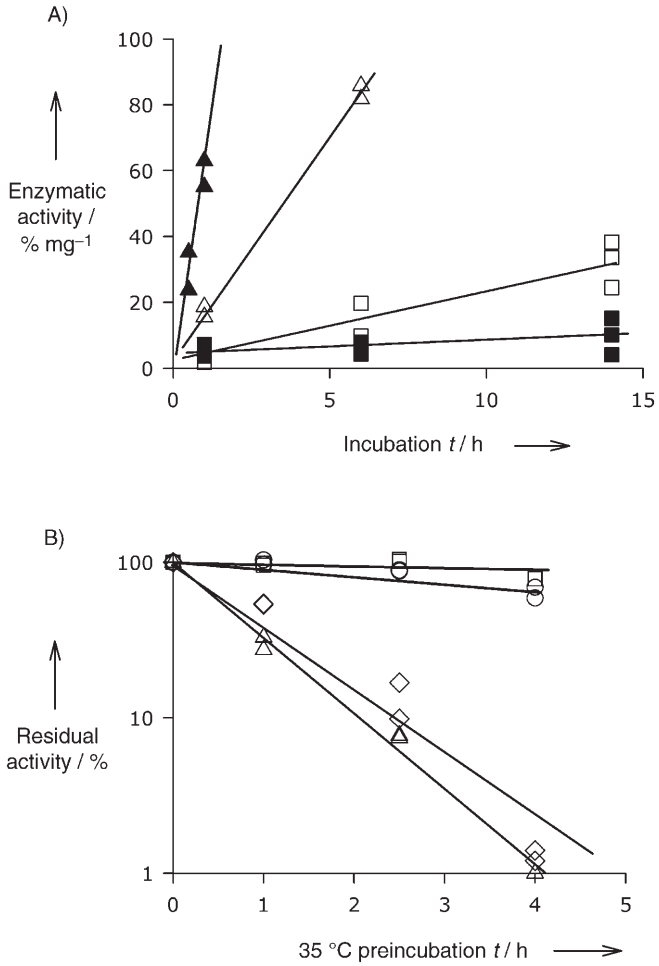

Figure 3. A) Effect of temperature on the enzymatic activity of mutants C457D–A525C and C457D–E526C. The percentage of labeled product per mg of protein produced by homogenates of mutant C457D–A525C at 25 °C (△) and 35 °C (▲) is compared with the percentage of labeled product per mg of protein produced by mutant C457D–E526C at 25 °C (□) and 35 °C (■). B) Residual enzymatic activity of mutants C457D (□), C457D–E526Q (○), C457D–E526C (◇), and C457D–E526A (△) after 1, 2.5, and 4 h of preincubation at 35 °C in the absence of substrate. After the preincubation the homogenates were incubated with substrate for 4 h at 25 °C.

Figure 4B, Ala525 stabilizes the conformation of the constriction loop through directed interaction of its backbone NH group with the side chain of the in-sequence-neighboring Asn523. We observe a conservative A→S mutation between the yeast and the human enzyme. In the yeast enzyme (Figure 4B) a water molecule can provide additional hydrogen-bonding interactions stabilizing the constriction loop; these interactions are present in the *Hsa*OSC because of the side-chain oxygen atom of the serine residue (Figure 4A). In the yeast mutant C457D–A525C the removal of a water molecule probably allows the same hydrogen-bonding pattern as in *Hsa*OSC (Figure 4C). The specific activity remains thus unchanged. In contrast to A525C, the mutation E526C dramatically influences specific activity. As can be seen from Figure 4B, Glu526 is the main contributor for the stabilization and linkage of at least three other tertiary structure elements of residues that are very distant in the sequence; however, only one of these linkages could be conserved in the E526C mutant (Figure 4D).

The observed specific activities at 35 °C and 25 °C (Table 2) of the three newly prepared mutants, designed to test the effect of the substitution of the glutamate at position 526 with glutamine, aspartate, or alanine, respectively, are in agreement with a structural role of Glu526, as proposed in the model of Figure 4. The substitution of the glutamate at position 526 with an uncharged amino acid having the same chain length, like glutamine, does not change the catalytic activity. From the hydrogen-bonding pattern depicted in Figure 4, we can argue that a simple change in the protonation state of His291, which is solvent-exposed, can allow glutamine to maintain the same stabilizing interaction pattern as glutamate. The shorter chain length of aspartate only does a suboptimal job in tertiary-structure stabilization, thus leading to a reduced specific activity in the C457D–E526D mutant. The substitution with alanine causes the same results already observed with cysteine: the specific activity is lower both at 35 °C and at 25 °C and the enzyme is not stable at 35 °C, as shown by the drop of residual activity after increasing times of preincubation at 35 °C in the absence of substrate (Figure 3B). When Glu526 is replaced by an alanine or cysteine residue, the hydrogen-bond linkage of different structural elements cannot be maintained, thereby resulting in a rather flexible arrangement of the tertiary structure around the constriction. For E526C, one should also consider that the increased steric bulk of the sulfur atom might lead to structural reorientations. It has been observed that the channel constriction loop must be mobile enough to rearrange upon passage of substrate or products[14, 15, 23] and this means that it needs a certain degree of flexibility. Such flexibility can allow the enlargement of the channel constriction by displacing the mobile loop as a consequence of the dissipation of energy produced by catalysis.[14] A higher flexibility that is constitutionally present because of a mutation can result in a less controlled process of substrate entering or product leaving or even in blockage of the constriction. The inactivation at 35 °C of the two mutants unable to maintain the hydrogen-bonding network of Glu526 strongly supports the assumption of structural reorientations. What kind of structural interactions are affected during the substrate/product-induced rearrangement because of flexibility is still an open question. We can speculate that, if a flexible channel loop is necessary for substrate/product-induced rearrangement, with higher flexibility the entrance could be blocked or unable to adjust to the substrate.

Effect of dodecyl-maleimide on *Sce*OSC mutants C457D, C457D–A525C, C457D–E526C, and C457D–E526A

The reactivity of mutants C457D–A525C and C457D–E526C to the thiol-reacting agent dodecyl-maleimide was compared with that of mutants C457D and C457D–E526A. As shown in Table 3, mutant C457D, which is devoid of a cysteine residue in the sequence of the hypothetical channel constriction, was only slightly affected by a high concentration of dodecyl-maleimide. Mutant C457D–A525C was inhibited at a concentration of 0.2 mM but not at a concentration of 0.025 mM, while

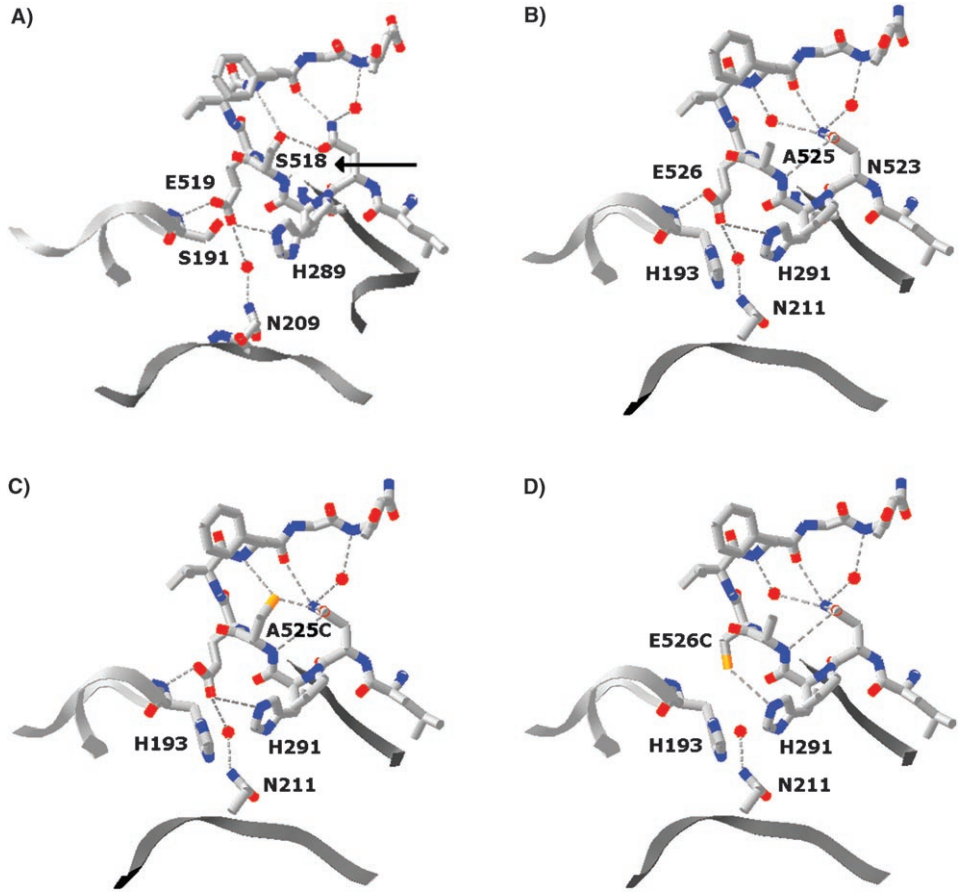

Figure 4. A) Hydrogen-bond interactions of Ser518 (equivalent to yeast Ala525) and Glu519 (equivalent to yeast Glu526) in the crystal structure of *Hsa*OSC. The side chain of the Glu526-equivalent residue links the section of the entrance constriction (indicated by an arrow, but actually above the plan of the drawing) through direct interactions to three, in-sequence-distant parts of the protein (ribbons in different shades of gray). B) Hydrogen-bond interactions of Ala525 and Glu526 in the model structure of *Sce*OSC. C) Hydrogen-bond interactions of the Ala525-replacement cysteine residue and Glu526 in the model structure of *Sce*OSC mutant A525C. D) Hydrogen-bond interactions of Ala525 and the Glu526-replacement cysteine residue in the model structure of *Sce*OSC mutant E526C. The most important interaction of the Ala525-equivalent residue in *Hsa*OSC is with Asn516 (corresponding to *Sce*OSC Asn523), which, in turn, is hydrogen bonded to three backbone residues of the constriction loop. The same pattern of interactions can be present in the *Sce*OSC A525C mutant (C), while in the wild-type yeast enzyme the stabilization of the constriction loop through the hydrogen-bonding pattern of the side chain of Asn523 can be achieved by an additional water molecule (B). The interaction pattern of the Glu526-equivalent residue in the crystal structure of *Hsa*OSC (A) is conserved in the homology model of *Sce*OSC (B), but disappears in the E526C mutant (D).

mutant C457D–E526C was still 45% inhibited by 0.01 mM dodecyl-maleimide.

Structural information allows interpretation of this experimental observation. As depicted in Figure 5, the solvent-exposed Connolly surface has been calculated in a hypothetical double mutant A525C–E526C: the sulfur atom of the cysteine residue in position 526 would have a much larger accessible surface (about 7 Å^2) than the sulfur atom of the cysteine in position 525 (<0.1 Å^2). This explains why C457D–E526C is already inhibited at very low concentrations (0.01 mM) of dodecyl-maleimide, whereas an inhibitory effect for C457D–A525C is only observed at much higher concentrations of dodecyl-maleimide.

The preincubation of the homogenates with dodecyl-maleimide in the absence of substrate showed that C457D–A525C and C457D–E526C were quickly and irreversibly inactivated in the first few minutes of preincubation in a concentration-dependent manner. In these time-dependent inactivation tests, we removed the dodecyl-maleimide after the preincubation, by adding a great excess (10 mM) of glutathione. Glutathione was proved to protect the enzyme from the inhibition in control experiments where the glutathione was mixed to the solution of dodecyl-maleimide before the addition of the homogenate: under these conditions, no inhibition of the enzy-

Table 3. Inhibition of the *Sce*OSC mutants by dodecyl-maleimide. Values are the means of duplicate assays of two different experiments.

[dodecyl-maleimide] / mM	Inhibition / % C457D	C457D–E526A	C457D–A525C	C457D–E526C
1	41.6 ± 4.0	n.d.[a]	86.0 ± 5.4	n.d.[a]
0.2	10.0 ± 4.1	9.0 ± 2.7	30.5 ± 3.0	89.6 ± 4.4
0.025	7.2 ± 1.3	0.0 ± 4.8	1.0 ± 0.2	74.7 ± 1.9
0.01	n.d.[a]	n.d.[a]	n.d.[a]	45.1 ± 6.4

[a] n.d. = not determined.

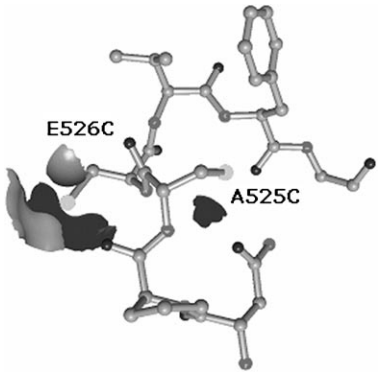

Figure 5. The picture shows the constriction loop of a hypothetical A525C–E526C double mutant. The solvent-exposed Connolly surface of the sulfur atoms of the two cysteines is shown as a shaded surface. The accessible surface of the sulfur atom of the residue in position 526 is at least 70 times larger than that of the residue in position 525.

matic activity was observed. The residual activity of mutant C457D–E526C dropped to 60% of the control levels after 2 min of preincubation with 0.01 mM dodecyl-maleimide and to 20% of the control levels with 0.025 mM dodecyl-maleimide, but it did not significantly decrease further after longer periods of preincubation. Similar results were obtained with mutant C457D–A525C: after 10 min of preincubation the residual activity dropped to 60% of the control levels with 0.2 mM dodecyl-maleimide and to 10% of the control levels with 1 mM dodecyl-maleimide. In both cases, at the lower concentration tested, there was no further increase of the inactivation by extending the preincubation time, possibly because of the exhaustion of dodecyl-maleimide by reaction with other thiols in the homogenate.

According to the results obtained with *Aac*SHC,[16] the inactivation of the enzyme by dodecyl-maleimide is mainly due to the presence of a cysteine residue in the hypothetical channel constriction or in a position involved in the constriction stabilization, since the C457D and C457D–E526A mutants are poorly affected by the inhibitor and only at high concentrations. The cysteine residues present in mutants C457D and C457D–E526A, belonging neither to the active site nor to the channel constriction, are perhaps less exposed to the thiol-reacting agent or, after reacting, do not significantly influence the enzymatic activity.

Conclusion

The presence in the *Sce*OSC of a channel constriction involving the amino acid residues from 523–532, highly conserved in all eukaryotic OSCs, is suggested by structural models based on homology with *Aac*SHC and *Hsa*OSC. In this region, Glu526 is very important to keep the functionality and stability of *Sce*OSC, since the mutants C457D–E526C and C457D–E526A, obtained by substituting the glutamate with cysteine or alanine residues, respectively, are not stable at 35 °C and are poorly active. The functionality of Glu526 is not due to the acidic function, since substitution with a glutamine residue affects neither the activity nor the thermal stability, but may possibly be due to the requirement for a side-chain length suitable to make stabilizing interaction, according to the *Hsa*OSC homology model. The mutants with cysteine residues at positions 525 and 526 are quickly and efficiently inactivated by the thiol-reacting agent dodecyl-maleimide, as a possible consequence of being localized, as in *Aac*SHC, in the channel of access of the substrate to the active site or involved in its stabilization by the formation a hydrogen-bonding network.

Experimental Section

Chemicals: All the components of buffers and cultural media and the bovine albumin used as a standard for protein determination were obtained from Sigma–Aldrich (Italy) unless otherwise specified. Molecular biology reagents were obtained from Promega Italia (Italy) unless otherwise specified. [2-^{14}C]acetate (55 mCi mmol^{-1}) was obtained from Amersham Pharmacia Biotech (UK). Squalene (S) and 2,3-oxidosqualene (OS) were prepared as previously described.[24] The labeled [^{14}C]squalene and [^{14}C]-(3*S*)-2,3-oxidosqualene were obtained through biological synthesis by incubating (*R*,*S*)-[2-^{14}C]mevalonic acid (1 μCi, 55 mCi mmol^{-1}, 2.04 GBq mmol^{-1}; Amersham Pharmacia Biotech, UK) with a pig liver S_{10} supernatant, in the presence of the OSC inhibitor U-14266A,[25] as previously described.[26] The synthesis of the thiol-reacting inhibitor dodecyl-maleimide has been described elsewhere.[19]

Yeast strains and culture conditions: The strains *Saccharomyces cerevisiae*, oxidosqualene cyclase mutant SMY8 (*MATa erg7::HIS3 hem1::TRP1 ura3–52-trpl-Δ63 leu2–3.112 his3-Δ200 ade2 Gal*$^+$), and SMY8[pSM61.21] (*MATa erg7::HIS3 hem1::TRP1 ura3–52-trpl-Δ63* ***leu2::OSC S. cerevisiae*** *his3-Δ200 ade2 Gal*$^+$) were kindly provided by Professor S. P. T. Matsuda (Department of Chemistry and Biochemistry and Cell Biology, Rice University Houston, TX, USA).[18]

SMY8 cells were grown to the early stationary phase at 30 °C in YPD medium (1% yeast extract, 2% peptone, 2% dextrose) supplemented with hemin (0.013 mg mL^{-1}) and ergosterol (0.02 mg mL^{-1}). Hemin is needed in the medium as the SMY8 strain contains a mutation (*hem1::TRP1*) affecting heme biosynthesis. The presence of a heme-mutant background is necessary for the viability of lanosterol synthase mutants in aerobic conditions.[18] SMY8 transformants were selected on synthetic complete media plates without leucine, containing yeast nitrogen base (0.67%), dextrose (2%), amino acids (0.2%), nitrogen base (0.5%), and agar (2%), supplemented with hemin (0.013 mg mL^{-1}) and ergosterol (0.02 mg mL^{-1}). SMY8 transformed with pSM61.21 plasmid derivatives were analyzed for ergosterol autotrophy by plating on YPG plates (1% yeast extract, 2% peptone, 2% galactose, 2% agar) supplemented with hemin (0.013 mg mL^{-1}).

Site-directed mutagenesis: The plasmid pSM61.21 (native *S. cerevisiae* OSC in the integrative galactose-inducible yeast expression vector pRS305Gal) was kindly donated by Professor S. P. T. Matsuda (Department of Chemistry and Biochemistry and Cell Biology, Rice University Houston, TX, USA).

To prepare the OSC mutant C457D, uracil-containing single-stranded DNA was prepared from phagemid pSM61.21 in *Escherichia coli* strain RZ1032 coinfected with M13K076 helper phage. Mutagenic oligonucleotide was used to prime the second strand synthesis with T4 polymerase and the DNA circle was closed with T4 ligase.[27] *E. coli* strain DH5α was transformed with the putative mutant construct,[27] and clones with the desired mutation were validated by DNA sequencing.

To prepare the double mutants C457D–A525C, C457D–E526C, C457D–E526D, C457D–E526Q, and C457D–E526A, uracil-containing single-stranded DNAs were prepared from phagemid pSM61.21 C457D.

Lithium acetate was used to transform the *S. cerevisiae* lanosterol synthase mutant SMY8 with all the constructs,[27] and transformed cells were selected on media plates as described above. Genomic DNA was isolated from yeast by using glass beads and phenol,[27] and the OSC mutant genes were amplified with PCR and sequenced.

DNA sequence analysis was carried out at the C.R.I.B.I.–BMR Servizio Sequenziamento DNA, Padova, Italy. Alignments were obtained with the MultiAlin program (http://prodes.toulouse.inra.fr/multalin/multalin.html).

Incorporation of [2-^{14}C]acetate into sterols: Ergosterol biosynthesis in whole recombinant yeast cells was measured by incorpora-

tion of [2-^{14}C]acetate into nonsaponifiable lipids, as previously described.[27] Briefly, yeast cells grown at 30 °C to early stationary phase were incubated with [2-^{14}C]acetate (0.2 mCi, 7.4×10^3 Bq, 55 mCi mmol^{-1}, 2.04 GBq mmol^{-1}) for 3 h at 30 °C. Cells were saponified in methanolic KOH for 1 h at 80 °C, and nonsaponifiable lipids were extracted with petroleum ether. The extract was spotted on TLC plates and developed in *n*-hexane/ethyl acetate (85:15). The separated components were identified by comparison with authentic standards of ergosterol, lanosterol, dioxidosqualene, oxidosqualene, and squalene. Radioactivity in separated bands was measured by collecting counts over a 5 min period with a System 200 imaging scanner. (Canberra Packard, USA)

Squalene and oxidosqualene cyclase activity: Cell-free homogenates were obtained as previously described.[28] Briefly, after lysis of the cell wall with lyticase the spheroplasts were homogenized with a Potter device. Proteins in the homogenate were quantified with a protein assay kit (Sigma), based on the method of Lowry modified by Peterson[29] and by using bovine serum albumin as a standard.

OSC activity was assayed as previously described.[30] Briefly, the homogenates were incubated with the labeled [^{14}C]-(3*S*)-2,3-oxidosqualene or [^{14}C]squalene (1000 cpm). The standard incubation time was 1 h at 35 °C, but different times and temperatures were used for some experiments as specified in the results. The enzymatic reaction was terminated by the addition of KOH in methanol, the lipids were saponified at 80 °C for 30 min, and the nonsaponifiable lipids were extracted with petroleum ether. Extracts were spotted on TLC plates with *n*-hexane/ethyl acetate (85:15) as the developing solvent. The conversion of the labeled substrate to labeled product was determined by using a System 200 imaging scanner.

Oxidosqualene cyclase inhibition: OSC inhibition was carried out by incubating the homogenates with the labeled [^{14}C]-(*3S*)-2,3-oxidosqualene (1000 cpm) in the presence of dodecyl-maleimide, as described above. Time-dependent inactivation of OSC was determined by adding the inhibitor in *N*,*N*-dimethylformamide (DMF) to the homogenate in the absence of substrate. Aliquots of preincubated homogenate were withdrawn at suitable intervals, transferred to test tubes containing labeled and unlabeled substrate 2,3-oxidosqualene (25 mM), Tween-80 (0.2 mg mL^{-1}), and Triton X-100 (1 mg mL^{-1}), and assayed for enzymatic activity as described above.

Residual activity was determined with respect to controls preincubated under the same conditions but in the absence of inhibitor. In the experiments of time-dependent inhibition, glutathione (10 mM) was added at the end of the preincubation period to remove residual inhibitor.

Computational methods

Hard- and software: Molecular modeling studies were performed on a Silicon Graphics Fuel R14000 Workstation. The software MOE 2004.03 (Chemical Computing Group Inc., Montreal, PQ, Canada) was used for sequence alignment, homology modeling, and structure-quality evaluation. Sequence-alignment scores were calculated with the ClustalX 1.83 program.[31] Modeling of mutants was carried out with the modeling package Moloc (Gerber Molecular Design, Basel, Switzerland). Final structures were minimized with Amber 7 (Scripps Institute, University of California, San Francisco, CA, USA).

Experimental data selection: Sequence information on yeast lanosterol synthase was taken from the Swiss-Prot database (accession number: P38604). The template structure for homology modeling, the crystal structure of human lanosterol synthase[15] was obtained from the Protein Data Bank[32] (PDB file code: 1W6K, resolution 2.1 Å). For building the homology model, water and octylglucoside molecules were removed from the structure.

Sequence alignment: The sequence alignment was done by using the MOE sequence alignment module with application of the BLOSUM 62 substitution matrix.[33] The alignment was checked for correct alignment of motifs and catalytic residues. There was no need to manually correct the resulting sequence alignment.

Homology modeling: Homology modeling was performed by using the homology modeling module of MOE. With the model sequence of yeast lanosterol synthase (Swiss-Prot accession number: P38604) and the template structure of human lanosterol synthase (PDB file code: 1W6K), MOE was set up to generate ten energy-minimized intermediate models. Different homologue models are the results of permutational selection of different loop candidates and side-chain rotamers. As a final model, the best intermediate model according to the MOE program's packing evaluation function was chosen and subsequent "fine" energy minimization (MOE default settings, RMS gradient of 0.005) of this model was performed. The stereochemical and structural quality of the resulting model was checked with the MOE program's protein-report utility. The report includes observed and statistically expected values of various measured bond lengths, angles, and dihedral values. The yeast lanosterol synthase model structure showed no significant deviation from the statistically expected values.

Minimization: The resulting model structure was refined by energy minimization by using the Amber 7.0 all-atom force field. Minimizations were carried out for 20 iterations of simplex minimization followed by 1500 steps of conjugate gradient minimization.[34]

Computational introduction of mutations: Mutants were manually introduced and energy minimized (constraint backbone atoms) with the Moloc software. The interaction pattern (hydrogen bonding, repulsion, water network) was also analyzed with the Moloc software. None of the introduced mutants led to steric or electronic repulsion and needed further refinement.

Acknowledgements

This work was supported by the Ministero dell'Istruzione, Università e Ricerca (MIUR), Italy (ex 60%). Thanks are due to Professor Seiichi Matsuda (Rice University, Houston, TX, USA) for supplying the plasmid pSM61.21 and the lanosterol synthase mutant SMY8 and for help with mutagenesis. Thanks are also due to Professor Giorgio Grosa (Università del Piemonte Orientale, Italy) for supplying the docecyl-maleimide inhibitor. T.S.-G. thanks her colleagues from Roche Biostructure in Basel, Switzerland, for providing the structural information on human oxidosqualene cyclase to the public domain, for stimulating discussions and for an overall supportive research atmosphere.

Keywords: cyclases · enzyme models · inhibitors · mutagenesis · steroids

[1] W. D. Nes, *Recent Adv. Phytochem.* **1990**, *24*, 283 – 327.
[2] I. Abe, M. Rohmer, G. D. Prestwich, *Chem. Rev.* **1993**, *93*, 2189 – 2206.

[3] K. U. Wendt, G. E. Schulz, E. J. Corey, D. R. Liu, *Angew. Chem.* **2000**, *112*, 2930 – 2952; *Angew. Chem. Int. Ed.* **2000**, *39*, 2812 – 2833.
[4] H. Dehmlow, J. D. Aebi, S. Jolidon, Y. H. Ji, E. M. von der Marck, J. Himber, O. Morand, *J. Med. Chem.* **2003**, *46*, 3354 – 3370.
[5] M. Mark, P. Müller, R. Maier, B. Eisele, *J. Lipid Res.* **1996**, *37*, 148 – 158.
[6] O. H. Morand, J. D. Aebi, H. Dehmlow, Y. H. Ji, N. Gains, H. Langsfeld, J. Himber, *J. Lipid Res.* **1997**, *38*, 373 – 390.
[7] B. Eisele, R. Budzinski, P. Müller, R. Maier, M. Mark, *J. Lipid Res.* **1997**, *38*, 564 – 575.
[8] G. R. Brown, D. M. Hollinshead, E. S. E. Strokes, D. S. Clarke, M. A. Eakin, A. J. Foubister, S. C. Glossup, D. Griffiths, M. C. Johnson, F. McTaggart, D. J. Mirrlees, G. J. Smith, R. Wood, *J. Med. Chem.* **1999**, *42*, 1306 – 1311.
[9] F. S. Buckner, J. H. Griffin, A. J. Wilson, W. C. van Voorhis, *Antimicrob. Agents Chemother.* **2001**, *45*, 1210 – 1215.
[10] J. C. Hinshaw, D.-J. Suh, P. Garnier, F. S. Buckner, R. T. Eastman, S. P. T. Matsuda, B. M. Joubert, I. Coppens, K. A. Joiner, S. Merali, T. E. Nash, G. D. Prestwich, *J. Med. Chem.* **2003**, *46*, 4240 – 4243.
[11] K. U. Wendt, K. Poralla, G. E. Schulz, *Science* **1997**, *277*, 1811 – 1815.
[12] A. Lenhart, D. J. Reinert, J. D. Aebi, H. Dehmlow, O. H. Morand, G. E. Schulz, *J. Med. Chem.* **2003**, *46*, 2083 – 2092.
[13] T. Schulz-Gasch, M. Sthal, *J. Comput. Chem.* **2003**, *24*, 741 – 753.
[14] D. J. Reinert, G. Balliano, G. E. Schulz, *Chem. Biol.* **2004**, *11*, 121 – 126.
[15] R. Thoma, T. Schulz-Gasch, B. D'Arcy, J. Benz, J. Aebi, H. Dehmlow, M. Hennig, M. Stihle, A. Ruf, *Nature* **2004**, *432*, 118 – 122.
[16] P. Milla, A. Lenhart, G. Grosa, F. Viola, W. A. Weihofen, G. E. Schulz, G. Balliano, *Eur. J. Biochem.* **2002**, *269*, 2108 – 2116.
[17] S. Lodeiro, M. J. R. Segura, M. Stahl, T. Schulz-Gasch, S. P. T. Matsuda, *ChemBioChem* **2004**, *5*, 1581 – 1585.
[18] E. J. Corey, S. P. T. Matsuda, C. H. Baker, A. Y. Ting, H. Cheng, *Biochem. Biophys. Res. Commun.* **1996**, *219*, 327 – 331.
[19] G. Grosa, F. Viola, M. Ceruti, P. Brusa, L. Delprino, F. Dosio, L. Cattel, *Eur. J. Med. Chem.* **1994**, *29*, 17 – 23.
[20] G. Balliano, G. Grosa, P. Milla, F. Viola, L. Cattel, *Lipids* **1993**, *28*, 903 – 906.
[21] E. J. Corey, H. Cheng, C. H. Baker, S. P. T. Matsuda, D. Li, X. Song, *J. Am. Chem. Soc.* **1997**, *119*, 1289 – 1296.
[22] I. Abe, M. Rohmer, *J. Chem. Soc.*, **1994**, 783 – 791.
[23] K. U. Wendt, A. Lenhardt, G. E. Schulz, *J. Mol. Biol.* **1999**, *286*, 175 – 187.
[24] M. Ceruti, G. Balliano, F. Viola, L. Cattel, N. Gerst, F. Schuber, *Eur. J. Med. Chem.* **1987**, *22*, 199 – 208.
[25] R. B. Field, C. E. Holmund, N. F. Whittake, *Lipids* **1979**, *14*, 741 – 747.
[26] M. Ceruti, G. Balliano, F. Rocco, P. Milla, S. Arpicco, L. Cattel, F. Viola, *Lipids* **2001**, *36*, 629 – 636.
[27] *Current Protocols in Molecular Biology* (Eds.: F. M. Ausubel, R. Brent, R. E. Kingston, D. D. Moore, J. G. Seidman, J. A. Smith, K. Struhl), Wiley, New York, **1999**.
[28] P. Milla, K. Athenstaedt, F. Viola, S. Oliaro-Bosso, S. Kohlwein, G. Daum, G. Balliano, *J. Biol. Chem.* **2002**, *277*, 2406 – 2412.
[29] G. L. Peterson, *Anal. Biochem.* **1977**, *83*, 346 – 356.
[30] S. Oliaro-Bosso, F. Viola, S. P. T. Matsuda, G. Cravotto, S. Tagliapietra, G. Balliano, *Lipids* ***2004****, 39*, 1007 – 1012.
[31] J. D. Thompson, T. J. Gibson, F. Plewniak, F. Jeanmougin, D. G. Higgins, *Nucleic Acids Res.* **1997**, *25*, 4876 – 4882.
[32] F. C. Bernstein, T. F. Koetzle, G. J. B. Williams, E. F. Meyer, Jr., M. D. Brice, J. R. Rodgers, O. Kennard, T. Shimanouchi, M. Tasumi, *J. Mol. Biol.* **1977**, *112*, 535 – 542.
[33] S. Henikoff, J. G. Henikoff, *Proteins* **1993**, *17*, 49 – 61.
[34] D. A. Case, D. A. Pearlman, J. W. Caldwell, T. E. Cheatham III, S. DeBolt, D. Ferguson, G. Seibel, P. Kollman, *Comput. Phys. Commun.* **1995**, *91*, 1 – 41.

Received: March 17, 2005
Published online on October 19, 2005

